A Low-cost Compliant 7-DOF Robotic Manipulator

Morgan Quigley, Alan Asbeck, and Andrew Ng

Abstract— We present the design of a new low-cost series-elastic robotic arm. The arm is unique in that it achieves reasonable performance for the envisioned tasks (backlash-free, sub-3mm repeatability, moves at 1.5m/s, 2kg payload) but with a significantly lower parts cost than comparable manipulators. The paper explores the design decisions and tradeoffs made in achieving this combination of price and performance. A new, human-safe design is also described: the arm uses stepper motors with a series-elastic transmission for the proximal four degrees of freedom (DOF), and non-series-elastic robotics servos for the distal three DOF. Tradeoffs of the design are discussed, especially in the areas of human safety and control bandwidth. The arm is used to demonstrate pancake cooking (pouring batter, flipping pancakes), using the intrinsic compliance of the arm to aid in interaction with objects.

I. INTRODUCTION

Many robotic manipulators are very expensive, due to high-precision actuators and custom machining of components. We propose that robotic manipulation research can advance more rapidly if robotic arms of reasonable performance were greatly reduced in price. Increased affordability can lead to wider adoption, which in turn can lead to faster progress—a trend seen in numerous other fields [1]. However, drastic cost reduction will require design tradeoffs and compromises.

There are numerous dimensions over which robotic arms can be evaluated, such as backlash, payload, speed, bandwidth, repeatability, compliance, human safety, and cost, to name a few. In robotics research, some of these dimensions are more important than others: for grasping and object manipulation, high repeatability and low backlash are important. Payload must be sufficient to lift the objects under study. Human-safety is critical if the manipulator is to be used in close proximity to people or in classroom settings.

Some areas of robotics research require high-bandwidth, high-speed manipulators. However, in many research settings, speed and bandwidth may be less important. For example, in object manipulation, service robotics, or other tasks making use of complex vision processing and motion planning, large amounts of time are typically required for computation. This results in the actual robot motion requiring a small percentage of the total task time. Additionally, in many laboratory settings, manipulator motions are often deliberately slowed to give the programmers time to respond to accidental collisions or unintended motions.

In this paper, we present a robotic arm with similar performance on many measures to high-end research robotic

Morgan Quigley, Alan Asbeck, and Andrew Ng are with the Department of Computer Science, Stanford University, Stanford, CA 94305, USA `mquigley, aasbeck, ang@cs.stanford.edu`
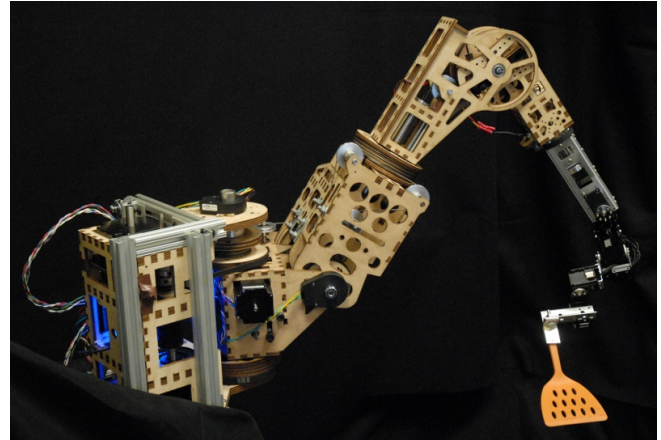
Fig. 1. The low-cost compliant manipulator described in this paper. A spatula was used as the end effector in the demonstration application described in this paper. For ease of prototyping, lasercut plywood was used as the primary structural material.

arms but at a drastically lower single-unit parts cost of $4135.

A shipped product must include overhead, additional design expenditures, testing costs, packaging, and possibly technical support, making a direct comparison with the parts cost of a research prototype rather difficult. However, we document the parts cost of our manipulator in order to give a rough idea of the possible cost reduction as compared to current commercially-available manipulators.

Our experiments demonstrate that millimeter-scale repeatability can be achieved with low-cost fabrication technologies, without requiring the 3-d machining processes typically used to construct robotic manipulators.

A set of requirements were chosen to ensure the arm would be useful for manipulation research:

- Human-scale workspace
- 7 Degrees of freedom (DOF)
- Payload of at least 2 kg (4.4 lb.)
- Human-safe:
    - Compliant or easily backdrivable
    - Flying mass under 4 kg
- Repeatability under 3 mm
- Maximum speed of at least 1.0 m/s
- Zero backlash

To meet these requirements at the lowest possible cost, a new arm design was developed. The arm uses low-cost stepper motors in conjunction with timing belt and cable drives to achieve backlash-free performance, trading off the cost of expensive, compact gearheads with an increased arm volume. To achieve human safety, a series-elastic design was

used, in combination with minimizing the flying mass of the arm by keeping the motors close to ground. The resulting prototype is shown in figure 1.

A brief outline of this paper is as follows. Section II gives an overview of other robotic arms used in robotics research. Section III gives an overview of the design of the arm, and discusses tradeoffs with its unique actuation scheme. Section IV discusses the series compliance scheme, and sections V, VI, and VII discuss the sensing, performance, and control, respectively. Section VIII discusses application of the robotic arm to a pancake-making task, followed by a conclusion.

II. RELATED WORK

A. Robotics research arms

There are a number of robotic arms used in robotics research today, many with unique features and design criteria. In this section, we discuss some recent widely-used and/or influential robotic arms.

The Barrett WAM [2], [3] is a cable-driven robot known for its high backdrivability and smooth, fast operation. It has high speed (3 m/s) operation and 2 mm repeatability.

The Meka A2 arm [4] is series-elastic, intended for human interaction; other, custom-made robots with series-elastic arms include Cog, Domo, Obrero, Twendy-One, and the Agile Arm [5], [6], [7], [8], [9]. The Meka arm and Twendy-One use harmonic drive gearheads, while Cog uses planetary gearboxes and Domo, Obrero, and the Agile Arm use ballscrews; the robots all use different mechanisms for their series elasticity. These arms have lower control bandwidth (less than 5 Hz) due to series compliance, yet that has not appeared to restrict their use in manipulation research. Several human-safe arms have been developed at Stanford using a macro-mini actuation approach, combining a series-elastic actuator with a small motor to increase bandwidth [10], [11].

The PR2 robot [12], [13] has a unique system that uses a passive gravity compensation mechanism, so the arms float in any configuration. Because the large mass of the arm is already supported, relatively small motors are used to move the arms and support payloads. These small motors provide human safety, as they can be backdriven easily due to their low gear ratios.

The DLR-LWR III arm [14], Schunk Lightweight Arm [15], and Robonaut [16] all use motors directly mounted to each joint, with harmonic drive gearheads to provide fast motion with zero backlash. These arms have somewhat higher payloads than the other arms discussed in this section, ranging from 3-14 kg. They are not designed for human safety, having relatively large flying masses (close to 14 kg for the DLR-LWR), although demonstrations with the DLR-LWR III have been performed that incorporate a distal force/torque sensor that uses the arm's high bandwidth to quickly stop when collisions are detected.

Of the robotic arms discussed previously, those that are commercially available are all relatively expensive, with end-user purchase prices well above $100,000 USD. However, there are a few examples of low-cost robotic manipulators used in research. The arms on the Dynamaid robot [17] are constructed from Robotis Dynamixel robotics servos, which are light and compact. The robot has a human-scale workspace, but a lower payload (1 kg) than the class of arms discussed previously. Its total cost is at least $3500 USD, which is the price of just the Dynamixel servos. In videos of it in operation, it appears to be slightly underdamped.

The KUKA youBot arm is a new 5-DOF arm for robotics research [18]. It has a comparatively small work envelope of just over $0.5\ m^3$, repeatability of 0.1 mm, and payload of 0.5 kg. It has custom, compact motors and gearheads, and is sold for 14,000 Euro at time of writing.

B. Robot arms using stepper motors

Many robot arms have been made using stepper motors. Pierrot and Dombre [19], [20] discuss how stepper motors contribute to the human-safety of the Hippocrate and Dermarob medical robots, because the steppers will remain stationary in the event of electronics failure, as compared to conventional motors which may continue rotating. Furthermore, they are operated relatively close to their maximum torque, as compared to conventional motors which may have a much higher stall torque than the torque used for continuous operation.

ST Robotics offers a number of stepper-driven robotic arms, which have sub-mm repeatability [21]. However, these are not designed for human safety. These are also relatively low-cost, for example the R17 arm (5-DOF, 0.75m workspace, 2 kg payload) is listed for $10,950 USD. Several other small, non-compliant robots were made in the 1980s-1990s used for teaching were also driven by stepper motors [22]. For example, the Armdroid robotic arm is 5-DOF and has 0.6m reach; it uses steppers with timing belts for gear reduction, then cables to connect to the rest of the arm [23].

III. OVERALL DESIGN

The arm has an approximately spherical shoulder and an approximately spherical wrist, connected by an elbow. The joint limits and topology were designed to enable the robot to perform manipulation tasks while being mounted near table-height, as opposed to anthropomorphic arms, which must hang down from the shoulder and require the base of the arm to be mounted some distance above the workspace. The shoulder-lift joint has nearly 180 degrees of motion, allowing the arm to reach objects on the floor and also work comfortably on tabletops. A summary of the measured properties and performance of the arm is shown in table I.

TABLE I

MEASURED PROPERTIES OF THE ARM

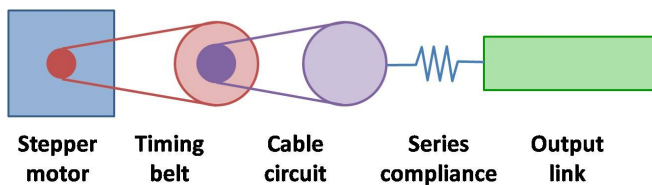| Length	1.0m to wrist
Total Mass	11.4 kg
Moving Mass	2.0 kg
Payload	2.0 kg
Max. speed	1.5 m/s
Repeatability	3 mm

Fig. 2. Actuation scheme for each of the proximal four DOF.

A. Actuation scheme

Figure 2 shows the actuation scheme for the proximal four DOF. These joints are driven by stepper motors, with speed reduction accomplished by timing belts and cable circuits, followed by a series-elastic coupling. Using only timing belts and cable circuits in the drivetrain results in low friction, minimal stiction, and zero backlash. This enables the arm to make small incremental motions (less than 0.5mm), and there is no gearing to damage under applied external forces. Combined with stepper motors, which have high torque at low speeds, this leads to a low-cost but relatively high performance actuation scheme. A downside to this scheme is that the reduction mechanisms occupy a relatively large volume, making the proximal portion of the arm somewhat large.

Using a two-stage reduction of timing belt followed by cable circuit accomplishes not only a larger gear reduction than a single stage, but also enables the motors to be located closer to ground. The motors for the two most proximal DOF are grounded, and the motors for the elbow and upperarm roll joints are located one DOF away from ground. By placing the relatively heavy stepper motors close to ground, the flying mass of the arm is greatly reduced: below the second (lift) joint, the arm is 2.0 kg. For comparison, a typical adult human arm is about 3.4 kg [24].

The two-stage reduction scheme leads to coupling between the motions of joints 1 and 2, and joints 2, 3, and 4. However, this coupling is exactly linear and can easily be estimated as a feedforward term in software. The routes of the timing belts and cables can be seen in figure 3. After the timing belts and cable circuits, the proximal four DOF have series elastic couplings between the cable capstan and the output link, discussed in section IV. These are used to provide intrinsic compliance to the arm, as well as providing force sensing (section V).

The distal three DOF are driven by Dynamixel robotics RX-64 servos. These joints do not have compliance aside from limiting the torques. However, the compliance of the proximal four DOF allows the end effector to be displaced in Cartesian space in three dimensions, barring kinematic singularities where only two dimensions will be compliant.

B. Tradeoffs of using stepper motors

Using stepper motors as actuators has a number of advantages. Stepper motors excel at providing large torques at low speeds, which is the target regime of the arm. They require a relatively low gear reduction, which can be accomplished with timing belts and cable drives. In the prototype
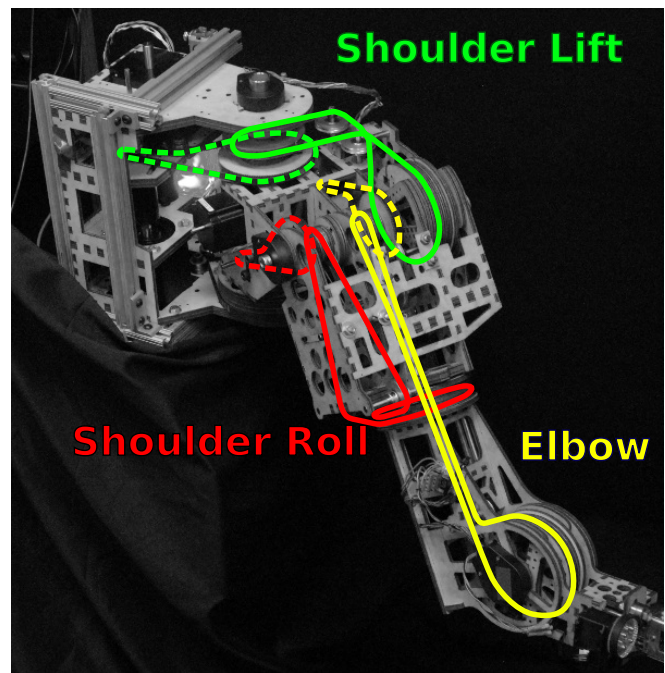

Fig. 3. Cable routes (solid) and belt routes (dashed) for the shoulder lift, shoulder roll, and elbow joints. All belt routes rotate about the shoulder lift joint. The elbow cables twist about the shoulder roll axis inside a hollow shaft. Best viewed in color.
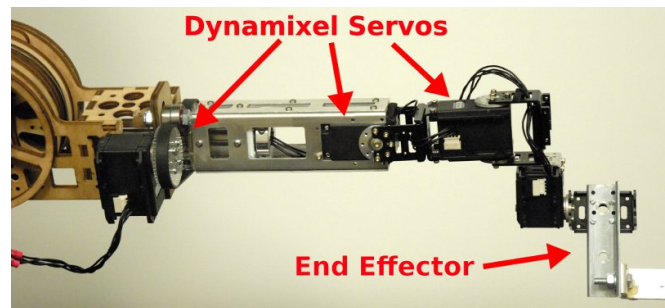

Fig. 4. Compact servos are used to actuate the distal three joints.

manipulator discussed in this paper, the effective reductions were 6, 10, 13, and 13, respectively, for the first four joints. DC motors, for comparison, generally require a significantly larger gear reduction through a gearbox that would be either susceptible to backlash or moderately expensive.

The stepper motors also act as electromagnetic clutches, improving safety if large forces are accidentally applied at the output. If a force is applied that causes a stepper to exceed its holding torque, the stepper motor will slip and the arm will move some distance until the force is low enough that the stepper can re-engage. The stepper holding torque is approximately 60% more than the maximum moving torque (and hence the maximum payload of the arm), large enough to avoid needlessly slipping but small enough to make the arm human-safe.

However, there are a few downsides of the steppers acting as an electromagnetic clutch. First, if a stepper motor slips, the arm may need to be re-calibrated. The arm uses joint-

angle encoders for state estimation, so closed-loop position control can still be done even after a slip, but force sensing will be miscalibrated (see section V). Second, the arm may move suddenly after a stepper motor slip. The arm only slips if relatively large amounts of force are applied, and after a slip the steppers initially provide little resistance. The moving arm may collide with other objects or people; this is mitigated by making the arm as light as possible. Adding backshaft encoders to the stepper motors would enable tracking of the motor position even during rotor slips, and enable faster stoppage of a slipping motor. Whether or not the additional cost is justified depends on the task and the anticipated frequency of unintended high-speed collisions. As envisioned, stepper slips occur only as a final layer of safety, and thus are not anticipated to be a frequent operational mode.

C. Hybrid SEA/non-SEA actuation scheme

The actuation scheme of the proposed manipulator uses series-elastic actuators (SEA) in the proximal 4 DOF, but non-series-elastic actuation for the distal 3 DOF. The bandwidth of the distal 3 DOF is somewhat higher than the bandwidth of the proximal 4 DOF, permitting a restricted set of higher-frequency motions. This is similar to that described in [25], which employs a macro-mini actuation scheme for the most proximal DOF and conventional actuators for the more distal DOF.

In our scheme, the lower three DOF still get most of the benefits of the series-elastic upper arm, including the ability to control forces by modulating a position. The main downside of this as compared to a full series-elastic scheme is that the gears in the distal DOF are more affected by shock loads, since (in the worst case) the mass of the entire arm is past the series compliance.

D. Arm inertia and series elastic stiffness

One important tradeoff with a series-elastic robot arm is the arm inertia and series elastic stiffness. Consider a one-DOF arm with moment of inertia I $[kg\,m^2]$ driven by a rotary joint with torsional stiffness k_θ $[N\,m/radian]$. The arm will oscillate at its natural frequency, which is $f_0 = \frac{1}{2\pi}\sqrt{k_\theta/I}$. If the arm has a low inertia or the series elastic coupling is stiff, the motor driving the arm may not have enough torque or bandwidth to compensate for this oscillation. Pratt and Williamson suggest increasing the arm's inertia to eliminate this effect [26]; other options are to reduce the spring constant; include damping in the series-elastic coupling; or increase bandwidth by decreasing the motor gear reduction, at the cost of a lower payload. For human-safe robotic arms with low inertia, this issue can be significant.

In our arm, considering the elbow joint, the natural frequency is around $f_0 = 5.1\ Hz$, with $k_\theta = 86\ N\,m/radian$ and $I = 0.083\ kg\,m^2$. This is close to the bandwidth of the motors with our current gear reduction.

E. Low-cost manufacturing

Several methods were used to achieve a low-cost design. The total cost of all of the stepper motors was $700. An

Motors	
Steppers	$700
Robotics servos	$1335
Electronics	$750
Hardware	$960
Encoders	$390
Total	$4135

alternative with comparable speed/torque performance is to use DC brushed motors with planetary gear reduction. Although they are available for a comparable price, their inexpensive gearheads exhibit more than 1 degree of backlash. High-performance gearheads or brushless motors would increase the cost by a factor of at least two. For example, a single zero-backlash harmonic drive actuator costs over $1000 USD, and a brushless planetary gearmotor of sufficient torque and 0.75-degree backlash costs $500 USD.

Lasercutting 5-ply plywood was used for most of the structure in the current prototype. The lasercutter used (Beam Dynamics OmniBeam 500, 500 Watts) can produce tolerances of 0.025mm, and excellent results were also achieved with an Epilog Legend Helix 24 (45 Watt) laser cutter. Dovetailing of the wood pieces was done, enabling them to be press-fit together, and flanged bearings and shafts were also press-fit into holes. It is unknown how the wood structure will respond to large temperature and humidity variations, but in a typical lab environment these are held relatively constant. Wood is an excellent material for rapid prototyping, and is rigid enough to meet the repeatability design requirements. In the future, we intend to make the complete structure out of folded sheet metal for a more durable structure. The lower arm of the robot was made of folded sheet metal as a first step in this direction. Folded metal structures cannot be made to the precision of custom-machined parts, but calibration techniques can be used to compensate for manufacturing errors.

The other technique used to keep costs low was to avoid all custom machining except for the lasercut structure; all other parts were off-the-shelf. A breakdown of the parts cost for the robot is shown in table II. Not included in this list are the costs of laser cutter time and assembly time; laser cutting would take 2.5 hours and assembly would take around 15 hours for additional copies of the arm.

IV. SERIES COMPLIANCE

The robot uses a compliant coupling in the proximal four joints. This provides increased human safety, allows the arm to be compliant even though the stepper motors are not backdrivable, and is used for force sensing as the deflection across the compliance is measured.

A diagram of the compliant coupling is shown in figure 5. Its operation is similar to the elastic couplings described in [27], [28], [29]. At the joint, a capstan used in the cable circuit (labeled **1** in figure 5) is suspended via bearings on the same shaft as the output link (**2**). The capstan is then
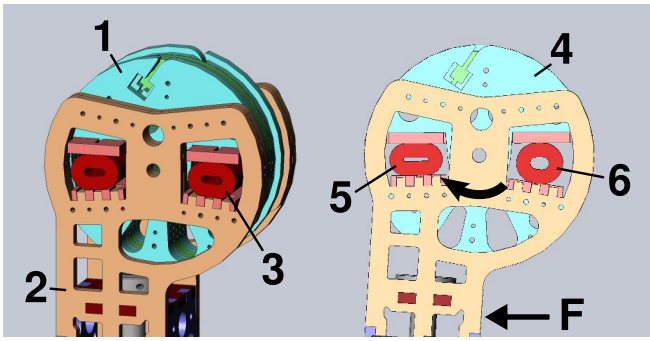
Fig. 5. Diagram of the series compliance. Left, compliant coupling with no external forces. Right, an applied force causes rotation.
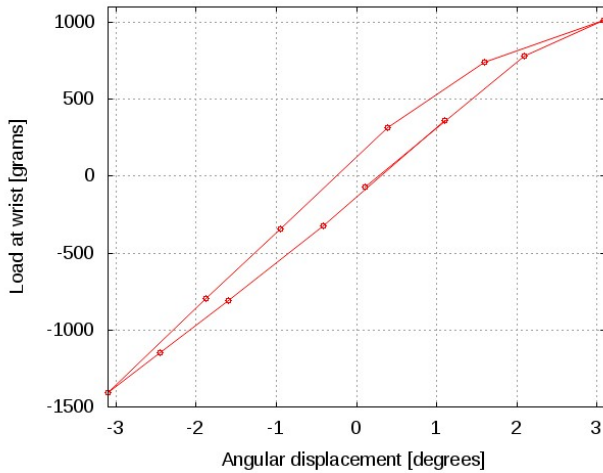

Fig. 6. Stiffness of the elbow. Some hysteresis is exhibited due to the polyurethane in the series compliance. The joint was quasi-statically moved through 70% of its normal operating range.

connected to the output link through the compliant element. Two plates connected to the output link extend through the middle of the capstan, which has two holes cut through the middle of it. Each hole contains a polyurethane tube (**3**), which is compressed between the plate from the output link and the side of the hole in the capstan. In figure 5(right), the capstan (**4**) is held stationary while an external force (**F**) is applied. This causes one polyurethane tube (**5**) to compress while the other (**6**) expands. The polyurethane tubes are initially pre-compressed to slightly more than half of their maximum possible compression so that they will always remain in compression as the output link moves with respect to the capstan.

Polyurethane was used to provide some mechanical damping of the joint, which gives the arm some hysteresis but helps eliminate oscillations. However, springs can readily be used in their place. Tubes were used instead of rods or balls to give the output links around 4 degrees of compliance in each direction, which requires several millimeters of travel. Figure 6 shows the stiffness and hysteresis of the compliant coupling in the elbow joint.

V. SENSING

As previously discussed, the first four joints of the manipulator are actuated by relatively large stepper motors embedded in the base and shoulder. The intrinsic stability of stepper motors forms a key aspect of the sensing strategy: assuming the stepper motors do not slip, the series of step motions the motors undergo can be precisely integrated to give the input displacement. Joint angles are measured directly using optical encoders. The deflection of the compliant element can thus be measured as the difference of the (post-reduction) motor position and the joint angle, thus permitting force sensing.

Integration of the motor step counts occurs on embedded microcontrollers in the first two links of the manipulator. This integration commences at power-up, and thus the motor step integration is best seen as a *relative* position estimate. To estimate the position offsets, enabling comparison with the (indexed) absolute joint-angle encoders, the manipulator is driven to the index pulses and held stationary. The stepper count when the manipulator is stationary at all encoder index pulses can be taken as a static offset to permit force-sensing calibration, barring hysteresis or plastic deformation of the compliant elements.

The distal three joints are actuated by Robotis Dynamixel RX-64 servos, which feature internal potentiometers with a usable range of 300 degrees. The potentiometer voltage is internally sampled by the servo.

To simplify the manipulator wiring, the stepper-motor drivers and servos share a common RS-485 bus. Sensors are sampled and actuators are commanded at 100 Hertz.

In the future, initial static pose estimation will be provided by accelerometers [30], enabling generation of safe trajectories to reach the encoder index pulses.

VI. PERFORMANCE

The arm's performance on several metrics was measured. Closed-loop repeatability was tested by moving the arm alternately between a home position and eight locations distributed around the workspace. The repeatability at the home position is shown in figure 7, where the position of the arm is plotted after it returned from each alternate location, as measured by an optical tracking system.

The encoders can register changes of 0.036 degrees, which corresponds to 0.64mm at the base joint with the arm fully extended. The stepper motor at the base joint can command changes of 0.52mm at the end effector. Moving down the arm, each subsequent motor can command sequentially finer motions due to increased effective gear ratios and shorter distances to the end effector.

Payload was measured by adding weights until the steppers slipped when slowly moving through the worst-case configuration. Maximum velocity was measured by commanding the fully-extended arm to move upwards at the maximum rate of the stepper controllers while observing the end-effector velocity with an optical tracking system. These experiments demonstrated a maximum payload of 2.0 kg and a maximum velocity of 1.5 m/s.
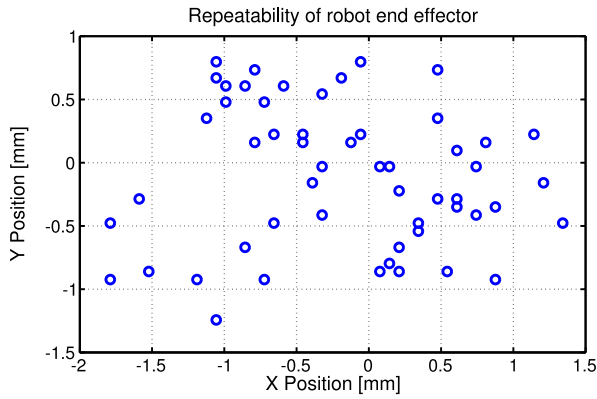
Fig. 7. Repeatability test results. The manipulator was repeatedly moved between a home position and one of 8 locations far apart in the workspace. This figure shows the position of the end effector after each round-trip to a distant location, as measured by an optical tracking system. Measurement accuracy is ± 0.1 mm.

Due to the ability of the encoders to register very small motions and the soft compliance of the arm, force sensing can be accomplished quite accurately by measuring the displacement of the arm. With the arm fully outstretched, masses as small as 15 grams reliably induce an angular deflection large enough to be measured by the shoulder-lift joint encoder.

VII. CONTROL AND SOFTWARE

The manipulator is controlled using standard techniques: closed-loop PID control in joint space is achieved using joint encoders. Inverse kinematics using the OROCOS-KDL library [31] allows cartesian control while respecting joint limits. Nullspace control is numerically computed on-the-fly using the Eigen C++ library [32]. Some of the joints are coupled due to the placement of heavy motors closer to ground. Linear feedforward terms were added to the joint-space controller to decouple the kinematics.

System integration and visualization is performed by the Robot Operating System (ROS) [33] under Linux to ease debugging. ROS supports hot-swapping software modules, and maganges the resulting setup and teardown of peer-to-peer data connections. It is thus possible to easily swap the underlying controller to support additional features, such as improved force sensing or to simulate Cartesian compliance.

All software and firmware used in this paper is available as BSD-licensed open-source software:
http://stanford-ros-pkg.googlecode.com

To demonstrate the ability of the manipulator to perform various tasks, we created a low-cost teleoperation system similar to that described in [34]. Compact, inexpensive USB devices containing MEMS inertial sensors and magnetometers were affixed to a shirt, allowing estimation of the posture of the teleoperator (figure 9), which in turn generated inverse-kinematics joint-angle targets. This software stack was used, among other things, to play a game of chess (figure 10) to demonstrate teleoperation involving fine motions. In order to avoid colliding with adjacent pieces when grasping, the end
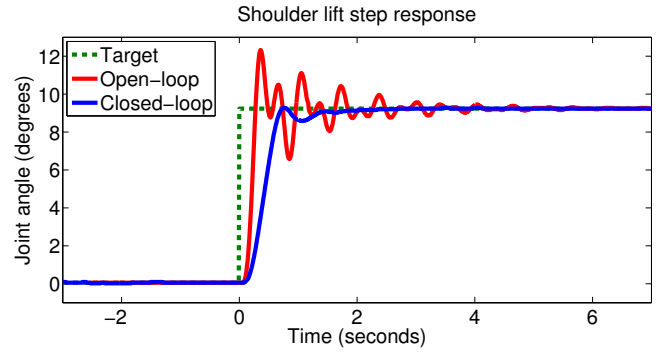
(a) The shoulder lift joint is coupled to the shoulder yaw joint. This results in non-sinusoidal open-loop ringing. However, this coupling can be corrected in software via a feed-forward term, allowing for rapid convergence of the closed-loop controller.
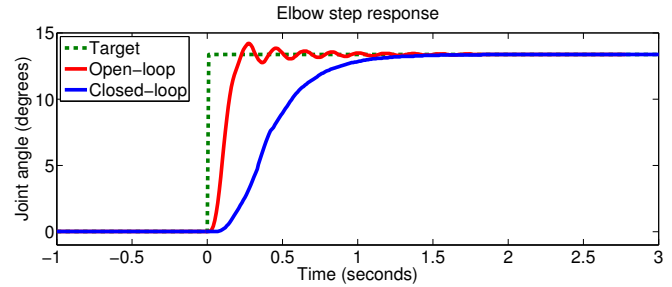
(b) The elbow tuning shown here is conservative, only seeking to match the bandwidth of the shoulder joints.
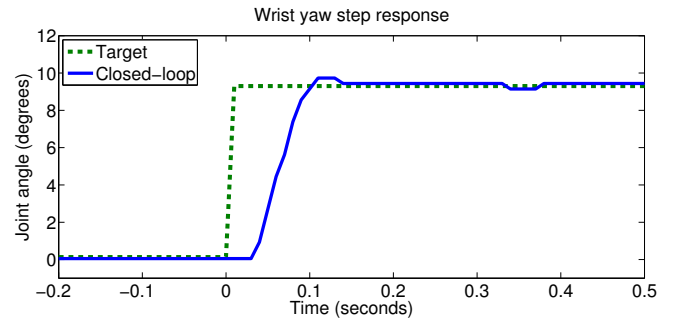
(c) The wrist joints are direct-driven from Robotis Dynamixel RX-64 servos, which are capable of relatively fast motions 360 degrees per second. Our implementation uses standard PID loops around the internal potentiometer readings.

Fig. 8. Step responses for each of the major types of actuators of the robot. Top, the shoulder-lift joint, a NEMA-34 stepper motor. Middle, the elbow joint, a NEMA-23 stepper motor. Bottom, the wrist yaw joint, a rigidly coupled Robotis RX-64 servo.

effector needed to move in spaces with only 2 centimeters of clearance.

VIII. APPLICATION

To explore the feasibility of real-world use of the proposed manipulator, we created a demonstration application of cooking pancakes. For this application, we affixed an end effector consisting of a distal roll axis connected to a spatula and spoon. The unpowered manipulator was moved by hand through a trajectory that scooped pancake batter out of a basin, poured two pancakes, flipped them, and finally deposited them on a plate (figure 11). Joint-space waypoints
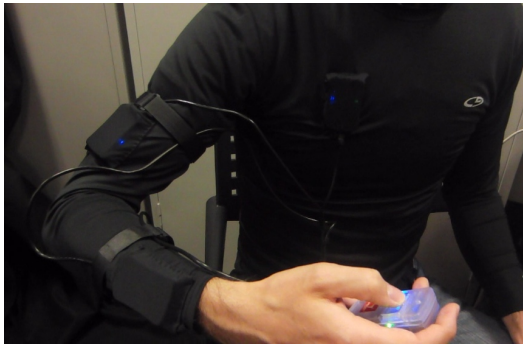
Fig. 9. Low-cost MEMS inertial sensors affixed to the teleoperator's torso, upper arm, lower arm, and hand to estimate desired end-effector positions.
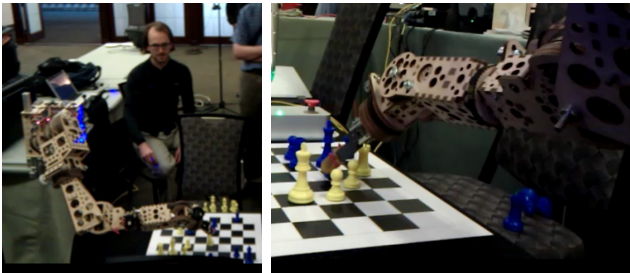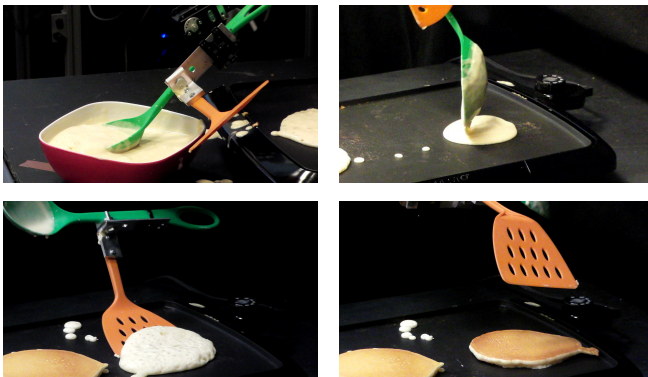

Fig. 10. Playing chess via teleoperation.

Fig. 11. Demonstration task: making pancakes (see video).

were recorded at key locations. The intrinsic compliance of the manipulator simplifed the necessary programming: only moving-setpoint control with linear joint-space interpolation was necessary in order to obtain reliable autonomous task completion, as shown in the video supplied with this paper. During the scraping operation, firm contact between the spatula and the grill surface was maintained by virtue of the series-elastic shoulder and elbow combined with the compliance of the spatula. As a result, neither high-bandwidth control nor accurate force/torque sensors were required at the end effector.

IX. CONCLUSIONS AND FUTURE WORK

A. Conclusions

We have presented the design of a low-cost robotic arm useful for manipulation research. In gearing, we traded off the space and complexity of a timing belt and zero-backlash cable drive circuit in place of the cost of an expensive gearhead. In motor selection, we used stepper motors for their high torque at low speeds, in exchange for a highly-reduced brushless or brushed motor. These design tradeoffs were chosen for the envisioned target application of robots interacting with unstructured environments such as a typical home or workplace, where the safety of intrinsic mechanical compliance is an important design consideration. The cost-controlling tradeoffs described in this paper were made as an effort towards designing affordable compliant manipulators, an area of research which, to date, has received little attention, and which we propose could have a large impact on the speed of adoption of robots into typical homes and workplaces.

B. Future Work

We intend to continue simplifying the mechanisms introduced in this paper, with the goal of enabling low-cost production of reasonable-performance manipulators. We intend to continue exploring low-cost fabrication techniques for functional components, and expect that many, if not all, structural components could be made with low-cost metalworking techniques, allowing fast assembly and easy maintenance, as well as reduced weight and increased stiffness.

REFERENCES

[1] C. Christensen, *The innovator's dilemma: when new technologies cause great firms to fail*. Harvard Business Press, 1997.
[2] B. Rooks, "The harmonious robot," *Industrial Robot: An International Journal*, vol. 33, no. 2, pp. 125–130, 2006.
[3] Barrett Technology, Inc., "WAM Arm," 2010. [Online]. Available: http://www.barrett.com/robot/products-arm-specifications.htm
[4] Meka Robotics, "A2 compliant arm," 2009. [Online]. Available: http://www.mekabot.com/arm.html
[5] R. Brooks, C. Breazeal, M. Marjanović, B. Scassellati, and M. Williamson, "The Cog project: Building a humanoid robot," *Computation for metaphors, analogy, and agents*, pp. 52–87, 1999.
[6] A. Edsinger-Gonzales and J. Weber, "Domo: A force sensing humanoid robot for manipulation research," in *2004 4th IEEE/RAS International Conference on Humanoid Robots*, 2004, pp. 273–291.
[7] E. Torres-Jara, "Obrero: A platform for sensitive manipulation," in *2005 5th IEEE-RAS International Conference on Humanoid Robots*, 2005, pp. 327–332.
[8] H. Iwata, S. Kobashi, T. Aono, and S. Sugano, "Design of anthropomorphic 4-dof tactile interaction manipulator with passive joints," *Intelligent Robots and Systems, 2005 (IROS 2005)*, pp. 1785 – 1790, Aug. 2005.
[9] J. Pratt, B. Krupp, and C. Morse, "Series elastic actuators for high fidelity force control," *Industrial Robot: An International Journal*, vol. 29, no. 3, pp. 234–241, 2002.
[10] M. Zinn, B. Roth, O. Khatib, and J. Salisbury, "A new actuation approach for human friendly robot design," *The international journal of robotics research*, vol. 23, no. 4-5, p. 379, 2004.
[11] D. Shin, I. Sardellitti, and O. Khatib, "A hybrid actuation approach for human-friendly robot design," in *IEEE Int. Conf. on Robotics and Automation (ICRA 2008), Pasadena, USA*, 2008, pp. 1741–1746.
[12] K. Wyrobek, E. Berger, H. der Loos, and J. Salisbury, "Towards a personal robotics development platform: Rationale and design of an intrinsically safe personal robot," in *Proc. IEEE Int. Conf. on Robotics and Automation*, 2008, pp. 2165–2170.

[13] Willow Garage, "PR2," 2010. [Online]. Available: http://www.willowgarage.com/pages/pr2/specs

[14] G. Hirzinger, N. Sporer, A. Albu-Schaffer, M. Hahnle, R. Krenn, A. Pascucci, and M. Schedl, "DLR's torque-controlled light weight robot III- Are we reaching the technological limits now?" in *Proceedings- IEEE International Conference on Robotics and Automation*, vol. 2, 2002, pp. 1710–1716.

[15] Schunk, "7-DOF LWA Manipulator," 2010. [Online]. Available: http://www.schunk-modular-robotics.com/left-navigation/service-robotics/components/manipulators.html

[16] R. Ambrose, H. Aldridge, R. Askew, R. Burridge, W. Bluethmann, M. Diftler, C. Lovchik, D. Magruder, and F. Rehnmark, "Robonaut: NASA's space humanoid," *IEEE Intelligent Systems and Their Applications*, vol. 15, no. 4, pp. 57–63, 2000.

[17] J. Stuckler, M. Schreiber, and S. Behnke, "Dynamaid, an anthropomorphic robot for research on domestic service applications," in *Proc. of the 4th European Conference on Mobile Robots (ECMR)*, 2009.

[18] KUKA, "youbot arm," 2010. [Online]. Available: http://www.kuka-youbot.com

[19] F. Pierrot, E. Dombre, E. Dégoulange, L. Urbain, P. Caron, S. Boudet, J. Gariépy, and J. Megnien, "Hippocrate: a safe robot arm for medical applications with force feedback," *Medical Image Analysis*, vol. 3, no. 3, pp. 285–300, 1999.

[20] E. Dombre, G. Duchemin, P. Poignet, and F. Pierrot, "Dermarob: a safe robot for reconstructive surgery," *IEEE Transactions on Robotics and Automation*, vol. 19, no. 5, pp. 876–884, 2003.

[21] S. Robotics, "R17 5-axis robot arm," 2010. [Online]. Available: http://www.strobotics.com/

[22] , "The Old Robots Web Site," 2010. [Online]. Available: http://www.theoldrobots.com/robot-robot.html

[23] Colne Robotics, "Armdroid," 1981. [Online]. Available: http://www.senster.com/alex_zivanovic/armdroid/index.htm

[24] R. Chandler, C. Clauser, J. McConville, H. Reynolds, and J. Young, *Investigation of inertial properties of the human body*. NTIS, National Technical Information Service, 1975.

[25] M. Zinn, O. Khatib, B. Roth, and J. Salisbury, "Playing it safe: A new actuation concept for human-friendly robot design," *IEEE Robotics & Automation Magazine*, vol. 11, no. 2, pp. 12–21, 2004.

[26] G. Pratt and M. Williamson, "Series elastic actuators," in *Proceedings of the IEEE/RSJ International Conference on Intelligent Robots and Systems (IROS-95)*, vol. 1, 1995, pp. 399–406.

[27] A. Kumpf, "Explorations in low-cost compliant robotics," Master's thesis, Massachusetts Institute of Technology, 2007.

[28] Y. Bar-Cohen and C. Breazeal, *Biologically inspired intelligent robots*. Society of Photo Optical, 2003.

[29] N. Tsagarakis, M. Laffranchi, B. Vanderborght, and D. Caldwell, "A compact soft actuator unit for small scale human friendly robots," in *IEEE International Conference on Robotics and Automation Conference (ICRA)*, 2009, pp. 4356–4362.

[30] M. Quigley, R. Brewer, S. Soundararaj, V. Pradeep, Q. Le, and A. Ng, "Low-cost Accelerometers for Robotic Manipulator Perception."

[31] H. Bruyninckx, "Open Robot Control Software: the OROCOS Project," in *IEEE International Conference on Robotics and Automation*, 2001, pp. 2523–2528.

[32] G. Guennebaud, B. Jacob, *et al.*, "Eigen v3," http://eigen.tuxfamily.org, 2010.

[33] M. Quigley, B. Gerkey, K. Conley, J. Faust, T. Foote, J. Leibs, E. Berger, R. Wheeler, and A. Ng, "ROS: an open-source Robot Operating System," in *Open-source Software Workshop of the International Conference on Robotics and Automation*, 2009.

[34] N. Miller, O. Jenkins, M. Kallmann, and M. Mataric, "Motion capture from inertial sensing for untethered humanoid teleoperation," in *2004 4th IEEE/RAS International Conference on Humanoid Robots*, 2004, pp. 547–565.